Langmuir

Article

pubs.acs.org/Langmuir

Determination of Effective Particle Density for Sterically Stabilized Carbon Black Particles: Effect of Diblock Copolymer Stabilizer Composition

David J. Growney,[†] Patrick W. Fowler,[†] Oleksandr O. Mykhaylyk,[†] Lee A. Fielding,[†] Matthew J. Derry,[†] Najib Aragrag,[‡] Gordon D. Lamb,[‡] and Steven P. Armes*[,†]

[†]Department of Chemistry, University of Sheffield, Brook Hill, Sheffield, South Yorkshire S3 7HF, U.K.

[‡]BP Formulated Products Technology, Technology Centre, Whitchurch Hill, Pangbourne, RG8 7QR, U.K.

Supporting Information

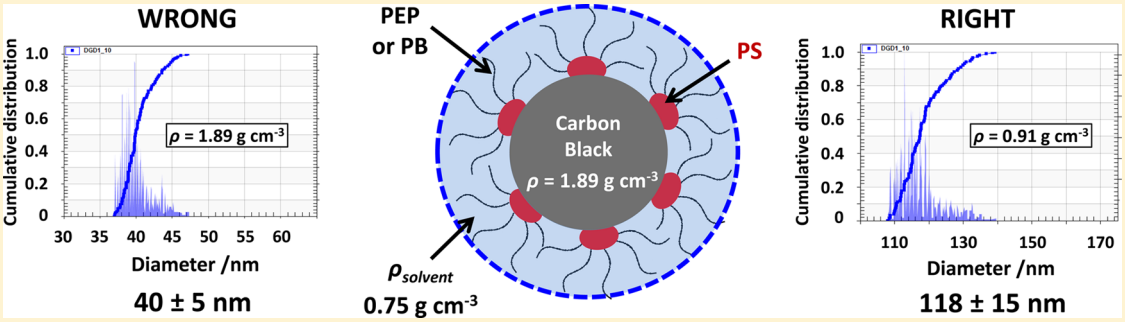

ABSTRACT: Two poly(styrene-*b*-hydrogenated isoprene) (PS-PEP) copolymers and a poly(styrene-*b*-hydrogenated butadiene) (PS-PB) diblock copolymer of differing polystyrene content (20, 28 or 35 mol %) and molecular weight (117−183 kg mol^{-1}) are examined. These copolymers form star-like micelles in *n*-dodecane, as judged by TEM, DLS, and SAXS studies. At ambient temperature, such micelles are known to adsorb intact onto a model colloidal substrate such as carbon black, conferring a high degree of dispersion (Growney, D. J.; Mykhaylyk, O. O.; Armes, S. P. *Langmuir* **2014**, *30*, 6047). Isotherms for micellar adsorption on carbon black at 20 °C are constructed using a supernatant depletion assay based on UV spectroscopy by utilizing the aromatic chromophore in the polystyrene block. Perhaps surprisingly, the diblock copolymer with the lowest polystyrene content has the strongest affinity for the carbon black particles. Assuming that the star-like diblock copolymer micelles adsorb onto carbon black to form hemi-micelles with a stabilizer layer thickness equal to the mean micelle radius, the effective particle density of the resulting sterically stabilized carbon black particles in *n*-dodecane can be estimated from the SAXS micelle dimensions based on geometric considerations. As an approximation, a spherical core−shell morphology was assumed, and the primary grain size of the carbon black particles was determined to be 74 nm diameter as judged by BET surface area analysis. Using this approach, effective particle densities of 0.90, 0.91, and 0.92 g cm^{-3} were calculated for sterically stabilized carbon black particles prepared using the PS-PB20, PS-PEP28, and PS-PEP35 diblock copolymers, respectively. These densities are significantly lower than that of carbon black (1.89 g cm^{-3}), which indicates that the sterically stabilized carbon black particles are substantially solvated. Since the rate of sedimentation of the sterically stabilized carbon black particles depends on the density difference between the effective particle density and that of *n*-dodecane (0.75 g cm^{-3}), particle size analysis via analytical centrifugation incurs large sizing errors unless the above corrected effective particle densities are utilized. This is important because analytical centrifugation is a highly convenient technique for assessing the relative degree of dispersion of sterically stabilized carbon black particles, which are utilized to inkjet inks and coatings formulations.

INTRODUCTION

The formation of colloidal aggregates on dissolution of an AB diblock copolymer in a solvent that is selective for one of the two blocks was first reported more than 50 years ago.[1,2] If the volume fraction of the soluble block is significantly greater than that of the insoluble block, then so-called "star-like" spherical micelles are formed in solution.[3−6] On the other hand, if the volume fraction of the soluble block is appreciably less than that of the insoluble block, then so-called "crew-cut" micelles can be obtained.[7−10] There are many papers describing the micellar self-assembly of wholly hydrophobic AB diblock copolymers in organic solvents.[3,11−15] In particular, polystyrene-based AB diblock copolymers that form polystyrene-core micelles in non-polar solvents such as *n*-alkanes are well documented.[16−23] These diblock copolymers can be readily prepared using classical anionic polymerization,[24,25] with the soluble block

Received: May 5, 2015
Revised: July 22, 2015
Published: July 23, 2015

DOI: 10.1021/acs.langmuir.5b01651
Langmuir 2015, 31, 8764−8773

typically being based on either polybutadiene, polyisoprene, or their hydrogenated derivatives.[17−19,26−30]

The adsorption of diblock copolymer micelles onto colloidal particles is well known.[31−36] For example, we recently reported that a commercial poly(styrene-*b*-hydrogenated isoprene) diblock copolymer adsorbs onto carbon black in the form of micelles from *n*-heptane, but as individual copolymer chains from chloroform (which is a good solvent for both blocks).[37] In related work, the adsorption of a star diblock copolymer onto the same carbon black particles revealed an interesting concentration-dependent flocculation/dispersion boundary, in which bridging flocculation was observed at low copolymer concentration but steric stabilization occurred at high copolymer concentration.[38] In both cases, carbon black was selected as a colloidal substrate for such studies because this material has been shown to be a convenient mimic for diesel soot particles.[36,39] The latter are formed during incomplete fuel combustion in diesel engines and are known to lead to long-term engine wear and reduced fuel economy.[40−42] Thus, suitable oil-soluble block copolymers that can minimize diesel soot formation and/or aid its dispersion on the nanometer scale are routinely added to engine oil formulations to address this problem and hence improve performance. In addition, sterically stabilized carbon black particles are widely used in inkjet formulations[43,44] and also as coatings.[45] Each of these applications requires fine control over the degree of dispersion of the carbon black particles, which is best assessed by determining accurate particle size distributions.

In the present study, we have investigated three polystyrene-based diblock copolymers of differing copolymer compositions and molecular weights. Their micellar self-assembly behavior in *n*-dodecane is examined, and the adsorption of these micelles onto carbon black particles dispersed in this solvent is studied at 20 °C.

The effective densities of the resulting sterically stabilized carbon black particles are calculated from geometric considerations, assuming (i) a spherical core−shell morphology and (ii) that the star-like diblock copolymer micelles form hemimicelles on the carbon black surface. Since the micelle layer thickness is relatively large compared to the primary grain size of the carbon black particles, such effective densities are significantly lower than that of carbon black alone. Thus, this approach is essential to determine accurate particle size distributions via analytical centrifugation, since otherwise substantial experimental errors are incurred. Analytical centrifugation is preferred to traditional particle sizing techniques such as dynamic light scattering. This is because fractionation occurs during the measurement, which leads to significantly higher resolution. In view of this advantage, the former technique has been utilized for the characterization of a wide range of colloidal dispersions.[46−55] Reliable particle size distributions can be obtained provided that the density of the particles and the continuous phase are known. Analytical centrifugation is particularly effective and convenient for hard spheres such as gold sols[54,56] but can also offer useful information for other colloidal particles. For example, this technique has been used to characterize polymer−silica nanocomposite particles with framboidal morphologies,[57,58] sterically stabilized latexes,[59,60] protein-coated particles,[61,62] core−shell latexes, emulsions,[63] and various organic/inorganic nanoparticles.[64−69]

EXPERIMENTAL SECTION

Materials. The three commercial polystyrene-based diblock copolymers used in this work were supplied by BP Formulated Products Technology (Pangbourne, U.K.). Such diblock copolymers can be prepared by living anionic polymerization of styrene with either butadiene or isoprene followed by catalytic hydrogenation using nickel-based catalysts.[36] This usually ensures well-defined diblock copolymers with minimal homopolymer contamination and relatively narrow molecular weight distributions.[25] Chloroform and *n*-dodecane solvents were obtained from Fisher Scientific UK Ltd. and were used as received. Deuterated chloroform for NMR studies was obtained from Goss Scientific Ltd., U.K. and was used as received. The carbon black (Regal 250R grade) was supplied by the Cabot Corporation (Billerica, MA, USA) and was used as received.

Gel Permeation Chromatography. The molecular weight distribution of the three diblock copolymers was assessed by gel permeation chromatography (GPC) using THF eluent. The THF GPC setup comprised two 5 μm "Mixed C" 30 cm columns, a Varian 290-LC pump, and a WellChrom K-2301 refractive index detector operating at 950 ± 30 nm. The THF mobile phase contained 2.0 v/v% triethylamine and 0.05 w/v% butylhydroxytoluene (BHT), and the flow rate was fixed at 1.0 mL min^{-1}. A series of ten near-monodisperse polystyrene standards (M_n = 580 to 552 500 g mol^{-1}) were used for calibration.

Dynamic Light Scattering (DLS). Temperature-dependent studies were performed using a Malvern Zetasizer NanoZS model ZEN 3600 instrument equipped with a Peltier cell and a 4 mW He−Ne solid-state laser operating at 633 nm at a fixed scattering angle of 173°. Copolymers were diluted in *n*-dodecane (0.01% w/w) and equilibrated for 5 min at 5 °C intervals in a 25−90−25 °C thermal cycle. The intensity-average diameter and polydispersity of the diblock copolymer star-like micelles were calculated at a given temperature by cumulants analysis of the experimental correlation function using Dispersion Technology Software version 6.20. Data were averaged over 13 runs, each of 30 s duration.

Transmission Electron Microscopy. Studies were conducted using a Phillips CM100 microscope operating at 100 kV on unstained samples prepared by drying a drop of dilute sample (approximately 0.01% w/w) on a carbon-coated copper grid.

Small-Angle X-ray Scattering. SAXS patterns were obtained for 1.0% w/w copolymer dispersions using a modified Bruker AXS Nanostar instrument (camera length = 1.46 m, Cu Kα radiation) equipped with a 2D HiSTAR multiwire gas detector. SAXS patterns were recorded over a q range of 0.008 Å^{-1} < q < 0.16 Å^{-1}, where $q = (4\pi/\lambda)\cdot\sin\theta$) is the length of the scattering vector and θ is half of the scattering angle. A glass capillary of 2 mm path length was used as a sample holder, and an exposure time of 2.0 h was utilized for each sample.

^{1}H NMR Spectroscopy. The mean polystyrene content of each diblock copolymer dissolved in a non-selective solvent ($CDCl_3$) was determined using a Bruker AV1-250 MHz NMR spectrometer (64 scans per spectrum). Variable-temperature spectra were recorded between 25 and 110 °C using d_{26}-dodecane with a Bruker AV1-400 MHz NMR spectrometer (32 scans per spectrum).

Helium Pycnometry. The solid-state density of Regal 250R carbon black was determined using a Micrometrics AccuPyc 1330 helium pycnometer at 20 °C.

Surface Area Analysis. BET surface area measurements were performed using a Quantachrome Nova 1000e instrument with dinitrogen gas (mean area per molecule = 16.2 Å^2) as an adsorbate at 77 K. Samples were degassed under vacuum at 100 °C for at least 15 h prior to analysis. The particle diameter, d, was calculated using the formula $d = 6/(\rho A_s)$, where A_s is the BET specific surface area in m^2 g^{-1} and ρ is the carbon black density in g m^{-3} obtained from helium pycnometry.

UV Spectroscopy. UV spectra were recorded at 20 °C for the diblock copolymers dissolved in 1:1 chloroform/*n*-dodecane mixtures (i.e., the *n*-dodecane supernatant was diluted with an equal volume of chloroform) using a PerkinElmer Lambda 25 instrument operating

DOI: 10.1021/acs.langmuir.5b01651
Langmuir 2015, 31, 8764−8773

Table 1. Summary of Copolymer Sample Codes, Copolymer Compositions, Molecular Weight Data, and Micelle Diameters for the Three Diblock Copolymers Used in This Work

						micelle diameter/nm[c]		
copolymer id	copolymer description	polystyrene content/mol %[a]	M_n/kg mol^{-1}[b]	M_w/kg mol^{-1}[b]	M_w/M_n[b]	TEM	SAXS	DLS
PS-PB20	poly(styrene-*b*-hydrogenated butadiene)	20	183	198	1.08	24	71	88
PS-PEP28	poly(styrene-*b*-hydrogenated isoprene)	28	117	121	1.04	24	68	85
PS-PEP35	poly(styrene-*b*-hydrogenated isoprene)	35	163	177	1.08	27	65	89

[a]Determined by ^{1}H NMR spectroscopy studies conducted in $CDCl_3$. [b]Determined by gel permeation chromatography (refractive index detector, THF eluent, calibration using a series of near mono-disperse polystyrene standards). [c]Determined at 20 °C after heating the initial copolymer dispersion in *n*-dodecane to 110 °C for 1 h. TEM "sees" only the micelle cores, whereas SAXS and DLS report the micelle cores plus the solvated micelle coronas.

between 200 and 500 nm. A calibration curve was constructed for the same copolymer dissolved in pure chloroform and gave a molar extinction coefficient of 222 ± 2 mol^{-1} dm^3 cm^{-1}, which is close to the literature value reported for polystyrene.[70] In order to determine the extent of copolymer adsorption onto carbon black via a supernatant depletion assay using UV spectroscopy, the following protocol was adopted. The desired mass of diblock copolymer (3.0−90.0 mg) was weighed into a glass vial, and carbon black (300.0 mg) was weighed into a separate vial. Then *n*-dodecane (5.00 mL) was added to the diblock copolymer, and this suspension was stirred at 20 °C (Turrax stirrer, 1 min) before being held at 110 °C for 1 h. The resulting copolymer micelle dispersion was added to the preweighed carbon black, stirred (Turrax stirrer, 1 min), sonicated for 1 h, and left on a roller mill for 16 h overnight. The dispersion was then centrifuged for 4 h at 18 000 rpm in a centrifuge rotor which was precooled to 15 °C so as to minimize solvent evaporation. Taking care not to disturb the sedimented carbon black particles, the supernatant was decanted into an empty vial and then 0.40 mL of this solution was diluted with an equal volume of pure chloroform to ensure molecular dissolution of the copolymer chains prior to analysis by UV spectroscopy. The aromatic chromophore at 262 nm due to the polystyrene block was used to quantify the copolymer concentration remaining in the supernatant after exposure to the carbon black using the Beer−Lambert linear calibration curve described above, thus enabling the adsorbed amount to be determined by difference.

Analytical Centrifugation. The LUMiSizer (LUM GmbH, Berlin, Germany) is a microprocessor-controlled analytical photocentrifuge that is particularly convenient for the analysis of the sterically stabilized carbon black dispersions described in this work. This instrument employs STEP technology (space- and time-resolved extinction profiles) to enable the measurement of the intensity of transmitted light as a function of time and position simultaneously over the entire cell length. The progression of the transmission profiles contains information on the rate of sedimentation and therefore allows calculation of the particle size distribution.[63]

Measurements were conducted at 20 °C on 1.0% w/w carbon black dispersions in *n*-dodecane at 3000 rpm using disposable polyamide cells (path length = 2 mm). The theoretical effective particle density of the sterically stabilized carbon black particles was calculated from geometric considerations (see later), and constant position analysis was used to determine volume-average particle diameters.

RESULTS AND DISCUSSION

Copolymer Characterization. The three commercial diblock copolymers used in this work are denoted by the sample codes indicated in Table 1. Polystyrene contents were determined to be 20, 28, and 35 mol % for PS-PB20, PS-PEP28, and PS-PEP35, respectively, using ^{1}H NMR spectroscopy in $CDCl_3$ at 20 °C (Figure S1 and Table 1). Each copolymer had a relatively narrow molecular weight distribution (M_w/M_n < 1.10) as judged by THF GPC analysis using a series of near mono-disperse polystyrene calibration standards. Unfortunately, each copolymer differs in terms of its copolymer molecular weight and block composition, which makes it impossible to examine the effect of either of these parameters in isolation. Nevertheless, an appropriate consideration of these three copolymers sheds useful light on their performance as dispersants for carbon black particles in non-polar media (see later).

Copolymer Self-Assembly. Micellization of the PS-PEP28 diblock copolymer has been extensively discussed elsewhere.[37] When dissolved directly in *n*-dodecane at 20 °C, ill-defined colloidal aggregates are obtained because the insoluble glassy polystyrene block prevents the efficient break-up of the original solid-state morphology of this copolymer. However, heating these aggregates to 110 °C for 1 h followed by cooling to 20 °C produces small, well-defined polystyrene-core micelles.[37] This morphological transformation is confirmed by transmission electron microscopy (TEM) studies of each of the three diblock copolymers before and after the 20−110−20 °C thermal cycle (Figure 1). Variable-temperature dynamic light scattering (DLS) was also used to monitor this change in copolymer morphology (Figure 2). The initial "sphere-equivalent" diameter observed at 25 °C should be treated with some caution since the TEM images revealed the presence of a significant fraction of polydisperse cylinders (Figure 1). On

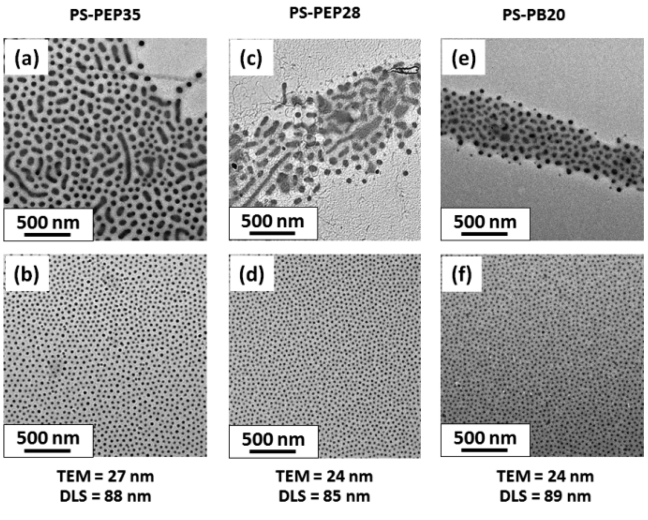

Figure 1. TEM images recorded for colloidal aggregates formed by the three linear polystyrene-based diblock copolymers used in this study. Images a−c show the relatively large, ill-defined non-equilibrium aggregates formed via direct dispersion at 20 °C in *n*-dodecane. In contrast, images d−f show the much smaller, well-defined equilibrium spherical micelles formed at 20 °C on heating this initial dispersion to 110 °C for 1 h in *n*-dodecane.

DOI: 10.1021/acs.langmuir.5b01651
Langmuir 2015, 31, 8764−8773

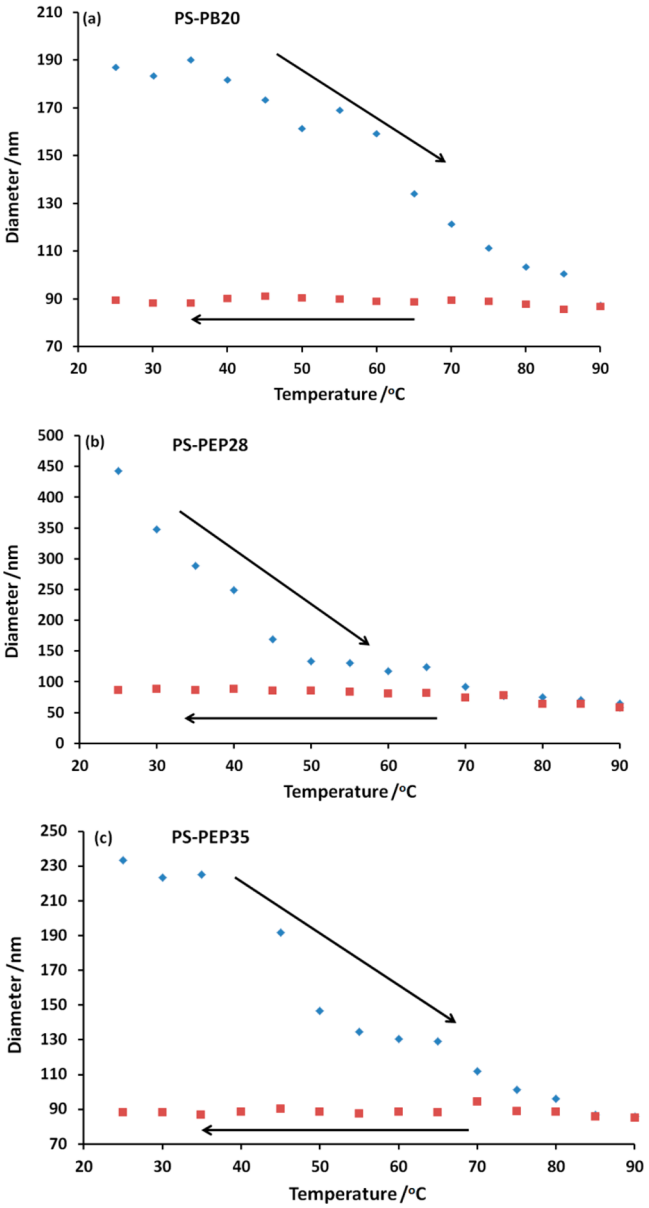

Figure 2. Variation in DLS intensity-average diameter observed for (a) PS-PB20, (b) PS-PEP28, and (c) PS-PEP35 diblock copolymer aggregates dispersed directly in *n*-dodecane at 25 °C, followed by heating to 90 °C (blue points) and cooling to 25 °C (red points). In each case this thermal cycle breaks up the initial large, ill-defined non-equilibrium aggregates and produces small, well-defined equilibrium micelles.

heating to 75 °C, the mean particle dimensions were dramatically reduced; this is consistent with the corresponding TEM images and indicates the formation of well-defined spherical micelles. It seems likely that the original cylinders are converted into spheres via a "budding" process since the intensity-average diameter of the small micelles is roughly comparable to the mean width of the original cylinders indicated by TEM (Figure 1). Similar observations were recently reported by Fielding et al.,[12] who observed a worm-to-sphere transition for poly(lauryl methacrylate)-poly(benzyl methacrylate) diblock copolymers on heating to above 90 °C in *n*-dodecane (as judged by TEM).

The three copolymers examined in this study form well-defined star-like micelles[21] with relatively constant core diameters of 24 to 27 nm, as judged by TEM (Table 1). After appropriate thermal treatment, DLS studies indicate overall micelle diameters of 85−89 nm. It is emphasized that TEM reports only the core diameter for the dried micelles, while SAXS and DLS report the overall hydrodynamic diameter of the solvated micelles (i.e., the micelle core plus the micelle corona). SAXS also provides additional structural information, which will be discussed later. To gain further insight into the mechanism of break-up of the ill-defined non-equilibrium aggregates and the subsequent formation of well-defined equilibrium micelles, variable-temperature ^{1}H NMR studies were conducted in d_{26}-dodecane. Figure 3 shows the partial ^{1}H

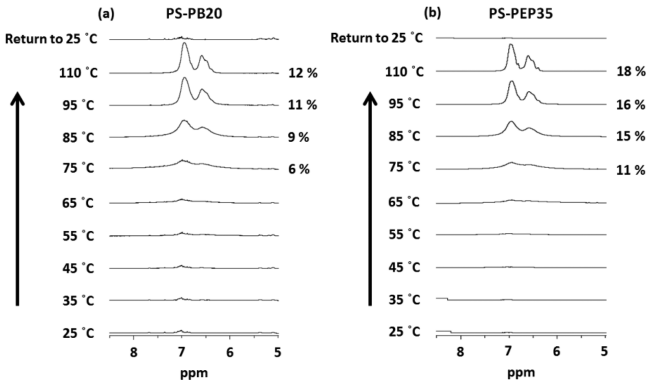

Figure 3. Partial ^{1}H NMR spectra recorded for (a) PS-PB20 and (b) PS-PEP35 in d_{26}-dodecane on heating from 25 to 110 °C followed by cooling to 25 °C. The appearance of aromatic signals at 6.5−7.0 ppm is attributed to increasing solvation of the polystyrene chains within the micelle cores at higher temperatures. Apparent polystyrene contents (mol %) are indicated on the right-hand side of each spectrum. The equivalent variable-temperature NMR study for PS-PEP28 in d_{26}-dodecane (and d_{16}-heptane) under the same conditions has been previously reported by Growney et al.[37]

NMR spectra recorded for PS-PB20 and PS-PEP35 copolymer dispersions in d_{26}-dodecane on heating to 110 °C followed by cooling to 25 °C. Initially, no ^{1}H NMR signals were observed between 25 and 65 °C. In contrast, broad aromatic signals characteristic of the core-forming PS block are observed in the 75 to 110 °C range, which subsequently disappeared on cooling back to 25 °C. Similar observations were recently reported for the PS-PEP28 copolymer by Growney et al.[37]

These spectroscopic observations suggest gradual solvent ingress within the micelle cores.[71] Such plasticization leads to a much lower effective T_g for the core-forming PS chains, which become increasingly mobile at elevated temperature. It is noteworthy that, if the apparent polystyrene contents in d_{26}-dodecane are compared to the actual polystyrene contents determined in $CDCl_3$ (which is a good solvent for both blocks), then the degree of solvation of the polystyrene block is never more than approximately 50−60% (Figure 3 and Figure S1). Such ^{1}H NMR spectra are therefore consistent with solvent-swollen micelle cores rather than molecularly-dissolved copolymer chains.

SAXS Studies of Copolymer Micelles. The star-like micelle model used to fit the three SAXS patterns shown in Figure 4 has been reported previously;[37] full details can be found in the Supporting Information. This model produced good fits to the SAXS patterns obtained for the PS-PB20, PS-PEP28, and PS-PEP35 diblock copolymer micelles formed in *n*-dodecane after thermal cycling (Figure 4 and Table S1).

DOI: 10.1021/acs.langmuir.5b01651
Langmuir 2015, 31, 8764−8773

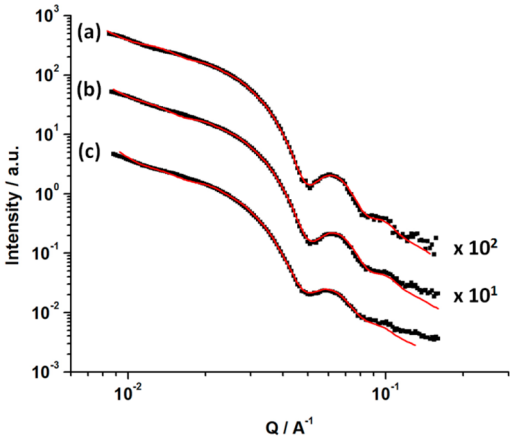

Figure 4. SAXS patterns obtained for 1.0% w/w diblock copolymer micelles in *n*-dodecane at 20 °C for (a) PS-PEP35, (b) PS-PEP28, and (c) PS-PB20. In each case well-defined micelles were obtained only after thermal annealing for 1 h at 110 °C (Figure 1). The patterns shown in a and b are multiplied by an appropriate arbitrary coefficient for the sake of clarity. The red lines represent fits to the SAXS data obtained using a star-like micelle model.[37,75]

Detailed SAXS analysis indicated a relatively low volume fraction of the *n*-dodecane solvent within the micelle cores (x_{sol} ≈ 0.10). Similar values have been reported by Pedersen et al. for a related diblock copolymer system.[72] This relatively low solvent volume fraction is consistent with the fact that *n*-dodecane is a non-solvent for polystyrene at 20 °C. Moreover, the star-like micelle model also indicated mean radii for the PS core (R_s) of 9.3 nm (PS-PB20), 8.9 nm (PS-PEP28), and 9.1 nm (PS-PEP35). The PB (or PEP) corona thicknesses (s) were found to be 26.4 nm (PS-PB20), 25.1 nm (PS-PEP28), and 23.2 nm (PS-PEP35). These data give overall particle diameters of 71 nm (PS-PB20), 68 nm (PS-PEP28), and 65 nm (PS-PEP35) (Table 2). These dimensions are within the same size range as those observed via DLS measurements. The largest micelle diameter is observed for PS-PB20, which is not unexpected given that this copolymer also has the highest molecular weight (183 K versus 117 K for PS-PEP28 and 163 K for PS-PEP35, see Table 1).

Carbon Black Characterization. In principle, understanding the adsorption of each commercial diblock copolymer onto carbon black should provide useful physical insights regarding their efficacy as putative diesel soot dispersants in engine oils. In this regard, carbon black acts as a convenient model colloidal substrate for genuine diesel soot since the latter is prohibitively expensive.[39] The physical properties of the Regal 250R carbon black used in this work have been previously characterized by Growney et al.:[37] it has a distinctive fractal morphology, which is typical of most carbon blacks and also diesel engine soot.[36,39,73,74] BET surface area analysis indicated a specific surface area of 43 m^2 g^{-1}, while helium pycnometry gave a solid-state density of 1.89 g cm^{-3}. Combining these values, the primary grain size for individual carbon black particles is calculated to be approximately 74 nm. This is in fairly good agreement with the number-average diameter of 70 nm estimated from TEM studies, with the BET value being considered to be more statistically robust.

Copolymer Adsorption on Carbon Black. Figure 5 shows the isotherms obtained for each diblock copolymer

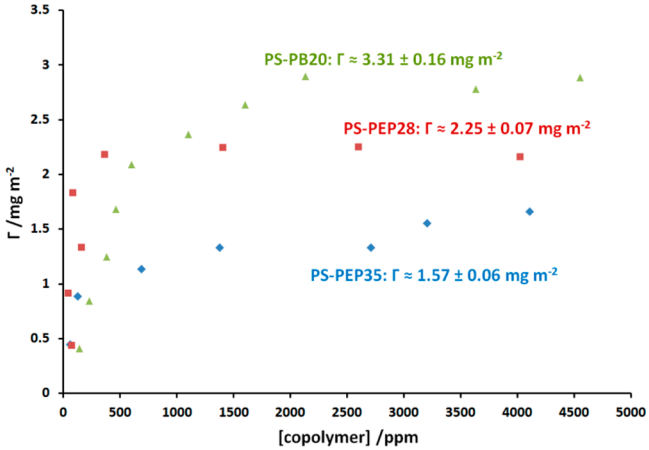

Figure 5. Langmuir-like adsorption isotherms obtained for the three polystyrene-based diblock copolymers (PS-PB20, PS-PEP28, and PS-PEP35) adsorbed in the form of well-defined micelles (obtained after heating to 110 °C for 1 h) onto carbon black particles from *n*-dodecane at 20 °C, as determined using a supernatant depletion assay based on UV spectroscopy. Equilibrium adsorbed amounts (Γ) are determined from the gradients of the corresponding linear plots for these isotherms (Figure S2).

adsorbed as well-defined micelles onto carbon black from *n*-dodecane at 20 °C. PS-PB20 exhibited the highest affinity isotherm with a maximum adsorbed amount, Γ, of 3.31 ± 0.16 mg m^{-2}, whereas PS-PEP28 and PS-PEP35 had Γ values of 2.25 ± 0.07 and 1.57 ± 0.06 mg m^{-2}, respectively (as determined from the gradients of the corresponding linear plots, see Figure S2 in the Supporting Information). Thus, increasing the polystyrene content of the copolymer leads to progressively weaker adsorption. This finding was not anticipated because Shar and co-workers[36] previously reported that the polystyrene component was essential for a strong interaction with the

Table 2. Summary of Steric Stabilizer Layer Thicknesses, Equilibrium Adsorbed Amounts of Diblock Copolymer Micelles on Carbon Black, Calculated Mass Fractions of the Carbon Black Core, Theoretical Effective Particle Densities, Density Differences (Δρ), and Volume-Average Particle Diameters Determined via Analytical Centrifugation for 1.0% w/w Carbon Black Dispersions at 20 °C (Using 6.0% w/w Copolymer Based on Carbon Black)[a]

copolymer id	steric stabilizer layer thickness, *d*, nm	adsorbed amount on carbon black, mg m^{-2}	mass fraction of carbon black core	effective particle density, ρ_{eff}, g cm^{-3}	density difference, Δρ, g cm^{-3}[b]	volume-average particle diameter, nm
PS-PB20	35.5	3.31	0.28	0.90	0.15	140 ± 10,[c] 163 ± 7[c]
PS-PEP28	34.0	2.25	0.29	0.91	0.16	118 ±15
PS-PEP35	32.5	1.57	0.31	0.92	0.17	117 ±10

[a]These tabulated data were calculated by assuming (i) a perfectly monodisperse spherical core−shell morphology, (ii) a primary grain size of 74 nm diameter for the carbon black particles, and (iii) the density of the steric stabilizer layer is equal to that of the pure solvent. [b]Δρ = effective particle density − density of *n*-dodecane. [c]Bimodal size distribution as judged by analytical centrifugation (Figure 8).

DOI: 10.1021/acs.langmuir.5b01651
Langmuir 2015, 31, 8764−8773

carbon black surface for adsorption from cyclohexane at 20 °C. On this basis, we had predicted that the highest-affinity isotherm would be observed for the diblock copolymer with the highest polystyrene content (i.e., PS-PEP35). However, both the copolymer molecular weight and chemical nature of the stabilizer block (PB or PEP) differ for all three copolymers (Table 1), so it is difficult to examine the effect of varying the polystyrene content under such circumstances. Presumably, subtle differences in the structure of these copolymers (and perhaps also the star-like character of the micelles) influence their adsorption behavior.

The resulting sterically stabilized carbon black dispersions were studied by TEM. Figure 6 shows representative images

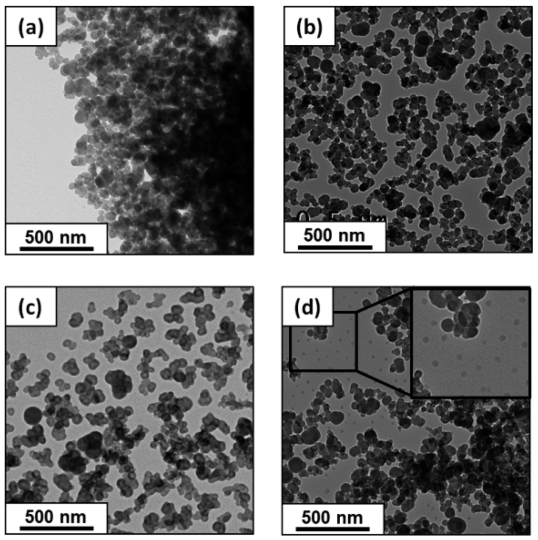

Figure 6. Representative TEM images for Regal 250R carbon black particles in *n*-dodecane: (a) no copolymer, (b) PS-PB20, (c) PS-PEP28, and (d) PS-PEP35. For b–d, 10% w/w copolymer based on carbon black was used in each case. TEM grids were prepared by allowing each copolymer dispersion to dry at 20 °C.

obtained for (a) the pristine carbon black and (b–d) dispersions stabilized using each copolymer in turn (at 10% copolymer by mass based on carbon black). Significantly smaller, more discrete carbon black particles are observed in the presence of each copolymer than for carbon black alone. Moreover, excess non-adsorbed micelles are observed for the dispersion prepared using PS-PEP35 (inset in Figure 6d). Inspecting the adsorption isotherms constructed for the three diblock copolymers in Figure 5, we find that this copolymer exhibited the lowest equilibrium adsorbed amount ($\Gamma = 1.57 \pm 0.06$ mg m^{-2}) and hence has a lower concentration threshold for the presence of excess micelles in solution. In contrast, PS-PEP28 and PS-PB20 each exhibit a stronger adsorption affinity for carbon black, which means that excess micelles are not present in solution under the same conditions.

Effective Densities of Sterically Stabilized Carbon Black Particles. In order to assess the degree of dispersion of sterically stabilized carbon black particles, analytical centrifugation has been used in combination with optical microscopy studies.[38] The latter technique is useful for assessing the presence of micrometer-sized agglomerates but is not sensitive to submicrometer-sized colloidal aggregates. In principle, analytical centrifugation should be capable of reporting high-resolution particle size distributions in the colloidal size range. However, the effective particle density must be known accurately for this technique since it is an essential input parameter. One important question here is whether the same effective particle density can be used regardless of the copolymer type. Alternatively, do the subtle differences in dimensions and adsorption behavior observed for the three types of copolymer micelles examined herein necessitate effective particle densities to be determined in each case? Since sedimentation is proportional to the particle mass and inversely proportional to the frictional force acting on the particle (which is a function of the particle morphology and size), the correct interpretation of sedimentation data requires a knowledge of the density of the sedimenting particles, which may be unknown for core–shell particles with solvated shells. Furthermore, for core–shell particles comprising differing densities for the core and shell components, it is known that an inherent density distribution is superimposed on particle size distributions determined by analytical centrifugation techniques. In the case where the shell density exceeds the core density, this leads to artifactual *narrowing* of the particle size distribution.[58] On the other hand, if the shell density is less than that of the core, which is the case in the present study, artifactual *broadening* of the particle size distribution is expected. In principle, this problem can be addressed by recalculating the true particle density for each data point of the digitized particle size distribution. For example, Fielding et al. reported a corrected particle size distribution obtained by disk centrifuge analysis of well-defined core–shell polystyrene/silica nanocomposite particles.[58] However, given the relatively ill-defined, highly fractal nature of the carbon black particles in the present work, such a correction has not been applied in this case.

For perfectly monodisperse spherical particles with a well-defined core–shell morphology, Lascelles and Armes derived a simple geometric relationship for the shell thickness, d, in terms of the core radius, R, and the mass fractions, m_1 and m_2, and densities, ρ_1 and ρ_2, of the core and shell components (eq 1).[64]

$$d = R\left[\left(\frac{m_2\rho_1}{m_1\rho_2} + 1\right)^{(1/3)} - 1\right] \quad (1)$$

Considering the relative volumes (V_1 and V_2) and mass fractions (m_1 and m_2) of a two-component composite material (in this case, core–shell particles) enables the calculation of a composite particle density, ρ_{comp}, using eq 2.

$$\rho_{comp} = \frac{m_1 + m_2}{V_1 + V_2} = \frac{m_1 + m_2}{\frac{m_1}{\rho_1} + \frac{m_2}{\rho_2}} \quad (2)$$

In the context of the present study, subscripts 1 and 2 refer to the carbon black core and copolymer micelle shell, respectively. If it is assumed that (i) the density of the copolymer shell is equal to that of the solvent (*n*-dodecane) and (ii) d corresponds to the mean radius of the star-like micelles calculated from SAXS analysis (Table 2), then a theoretical effective particle density can be calculated for sterically stabilized carbon black particles. However, we emphasize that this approach is only an approximation since it assumes a monodisperse spherical morphology for carbon black, which is clearly not the case (Figure 6). In addition, it is assumed that the star-like diblock copolymer micelles adsorb to form a hemimicelle at the surface of the carbon black particles whose mean thickness is equal to that of the original micelle radius[37] and

DOI: 10.1021/acs.langmuir.5b01651
Langmuir 2015, 31, 8764–8773

that furthermore the density of this copolymer stabilizer shell approximates to that of the pure solvent (which is 0.75 g cm^{-3} for *n*-dodecane at 20 °C). This situation is depicted schematically in Figure 7.

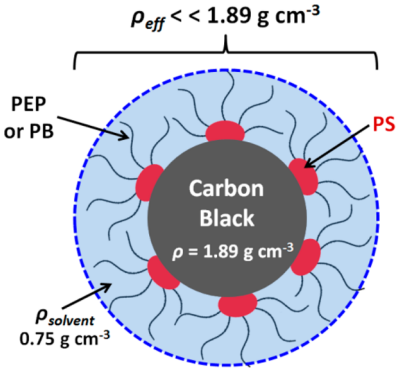

Figure 7. Schematic representation of the sterically stabilized carbon black particles for which the effective particle density, ρ_{eff}, is calculated using simple geometric considerations based on the micelle dimensions as determined by SAXS (Tables 1 and 2). In reality, these carbon black particles exhibit a fractal morphology rather than the spherical core–shell morphology shown here.

Using eqs 1 and 2 in combination with the SAXS micelle dimensions and carbon black primary grain size derived from BET surface area analysis, effective particle densities of 0.90, 0.91, and 0.92 g cm^{-3} were calculated for sterically stabilized carbon black particles prepared using PS-PB20, PS-PEP28, and PS-PEP35 copolymer micelles, respectively (Table 2). Clearly, these theoretical values are substantially lower than the solid-state density of carbon black indicated by helium pycnometry (1.89 g cm^{-3}). This indicates that the mass fraction of the low-density stabilizer shell (which can be approximated as comprising pure solvent) is significantly larger (~70%) than that of the high-density carbon black cores (Table 2).

Stokes' law can be used to calculate particle velocities for such sterically stabilized carbon black particles in pairs of similar solvents, such as *n*-dodecane and *n*-decane or *n*-dodecane and deuterated *n*-dodecane.[38] In principle, such particle velocities can be used to calculate the effective particle density. However, in practice this approach is not valid if the shell component dominates the core component since the density of the solvent shell necessarily varies with the nature of the solvent, which in turn leads to significantly different effective particle densities. In view of this technical problem, approximate effective particle densities were instead calculated purely on the basis of geometric considerations.

Particle size analysis via analytical centrifugation using the LUMiSizer instrument utilizes eq 3.

$$x^2 = \frac{18\eta_F}{(\rho_P - \rho_F)\omega^2 t} \ln\left(\frac{r_m}{r_0}\right) \quad (3)$$

Here x is the particle diameter, η_F is the viscosity of the spin fluid, ρ_P is the density of the sedimenting particles, ρ_F is the density of the spin fluid (in this case, *n*-dodecane), ω is the angular velocity, t is the sedimentation time, r_m is an arbitrary (fixed) position of the measurement of light transmission, and r_0 is the position of the solvent meniscus.

The form of eq 3 (or more specifically, the density difference term, $\rho_P - \rho_F$) indicates that huge errors (~300%) are incurred if the solid-state density of carbon black is erroneously used as an input parameter for determining volume-average particle size distributions via analytical centrifugation. This important point is emphasized in Figure 8, which shows the apparent and actual volume-average particle size distributions determined for the three types of sterically stabilized carbon black particles using (a) the density of carbon black alone and (b) the effective particle densities calculated using eqs 1 (see Table 2) and 2. In the former case, the particle size distributions are clearly too low since the volume-average diameter is less than the primary grain size of the carbon black particles (74 nm as judged by BET surface area analysis and confirmed by TEM studies). In contrast, physically reasonable volume-average diameters (117–140 nm) are obtained when using effective particle densities that account for the relatively high degree of solvation for such particles.

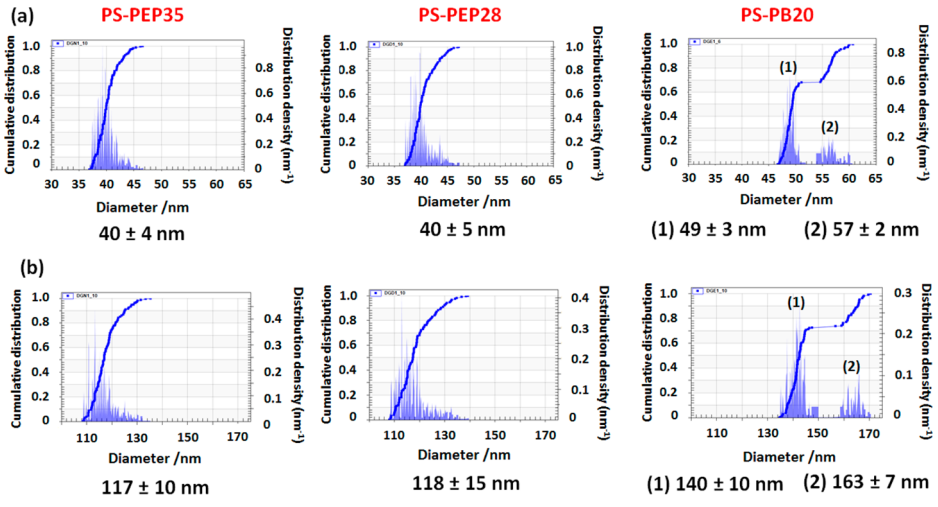

Figure 8. Particle size distributions obtained via analytical centrifugation analysis of 1.0% w/w carbon black particles dispersed in *n*-dodecane at 20 °C with the aid of the three diblock copolymers used in this work (PS-PB20, PS-PEP28, and PS-PEP35). Volume-average diameters are calculated (a) using the solid-state density of carbon black (which leads to large experimental errors) and (b) using theoretical effective particle densities (Table 2). In each case, 6.0% w/w copolymer was utilized on the basis of the mass of carbon black. Instrument conditions: 3000 rpm for 166 min.

DOI: 10.1021/acs.langmuir.5b01651
Langmuir 2015, 31, 8764–8773

The effect of varying the solvated stabilizer layer thickness (d) on the density difference ($\Delta\rho$) between the particles and the solvent for sterically stabilized carbon black particles dispersed in *n*-dodecane at 20 °C is plotted in Figure S3. This relationship was calculated using eqs 1 and 2 by assuming (i) a perfectly monodisperse spherical core−shell morphology, (ii) a primary grain size of 74 nm diameter for the carbon black particles, and (iii) that the density of the steric stabilizer layer is equal to that of the pure solvent. Although changes in $\Delta\rho$ are particularly large for relatively thin stabilizer layers (<10 nm), it is noteworthy that the density difference ($\Delta\rho$) remains quite sensitive to the solvated steric stabilizer layer thickness within the range of interest (32.5−35.5 nm, see Table 2). This highlights the importance of calculating accurate effective particle densities for such sterically stabilized carbon black dispersions.

Effect of Diblock Copolymer Composition on Carbon Black Dispersion Stability. It is perhaps worth mentioning that, despite the comparable dimensions of the copolymer micelles in solution (Table 1), their differing adsorption behavior (Figure 5) leads to subtle differences in the effective particle density for the corresponding sterically stabilized carbon black particles (Table 2). However, the volume-average particle size distributions obtained for these dispersions are broadly comparable (Figure 8). This indicates that each diblock copolymer leads to a similar degree of dispersion for carbon black in *n*-dodecane at 20 °C. Hence, all three copolymers are expected to be useful dispersants for diesel engine soot in engine oils.

CONCLUSIONS

Three near mono-disperse polystyrene-based diblock copolymers each form large, ill-defined polydisperse colloidal aggregates when dissolved directly in *n*-dodecane at 20 °C. However, a single heating cycle (110 °C, 1 h) breaks up such aggregates, leading to the formation of well-defined spherical micelles on cooling to 20 °C. Variable-temperature ^{1}H NMR studies conducted in d_{26}-dodecane are consistent with these observations, since partial solvation of the core-forming polystyrene chains is observed above 65 °C. Dynamic light scattering studies also confirmed a gradual reduction in the intensity-average diameter at higher temperature for all three diblock copolymers, followed by the formation of small near mono-disperse micelles on cooling to 20 °C. The adsorption of such micelles onto carbon black particles, which serve as a convenient mimic for diesel soot, was quantified using a supernatant depletion assay based on UV spectroscopy. Maximum adsorbed amounts, Γ, corresponding to micelle monolayer formation, were determined to be 3.31, 2.25, and 1.57 mg m^{-2} for PS-PB20, PS-PEP28, and PS-PEP35. Thus, increasing the mole fraction of the polystyrene anchor block actually leads to weaker micelle adsorption at the surface of the carbon black particles.

Assuming a spherical core−shell morphology, effective particle densities were calculated for the three types of sterically stabilized carbon black particles using (i) the micelle dimensions derived from SAXS and (ii) the primary grain size of the carbon black determined by BET surface area analysis. This approach yielded effective particle densities of 0.90, 0.91, and 0.92 g cm^{-3} for the sterically stabilized carbon black particles prepared using the PS-PB20, PS-PEP28, and PS-PEP35 diblock copolymers, respectively. Thus, although these three copolymers form micelles in *n*-dodecane with rather similar dimensions, each copolymer actually leads to a subtly different effective particle density, which is always substantially lower than the solid-state density of carbon black (1.89 g cm^{-3}). Since the rate of sedimentation of the sterically stabilized carbon black particles depends on the density *difference* between the effective particle density and the *n*-dodecane solvent (density = 0.75 g cm^{-3}), substantial errors can be incurred in analytical centrifugation studies unless appropriate care is taken to determine an accurate effective particle density. This is important because analytical centrifugation is a highly convenient technique for assessing the relative degree of dispersion of sterically stabilized carbon black particles by comparing their volume-average particle size distributions. Overall, this study has enhanced our understanding of the performance of three commercial diblock copolymers when employed as diesel soot dispersants in engine oil formulations. Given the wide range of applications for sterically stabilized carbon black dispersions, our results are likely to have broader implications.

ASSOCIATED CONTENT

Supporting Information

The Supporting Information is available free of charge on the ACS Publications website at DOI: 10.1021/acs.langmuir.5b01651.

^{1}H NMR spectra ($CDCl_3$) and THF GPC curves for the three copolymers, details of the star-like micelle SAXS model, a summary table of SAXS structural parameters for the copolymer micelles, linear plots for the three copolymer adsorption isotherms, effect of varying the steric stabilizer layer thickness on the density difference between the effective particle density and the solvent for sterically-stabilized carbon black particles in *n*-dodecane at 20 °C. (PDF)

AUTHOR INFORMATION

Corresponding Author

*E-mail: s.p.armes@shef.ac.uk.

Notes

The authors declare no competing financial interest.

ACKNOWLEDGMENTS

We thank BP Formulated Products Technology for funding a Ph.D. studentship for D.J.G. We also thank Dr. D. Fomitchev of Cabot Plastics for the donation of the Regal 250R carbon black particles.

REFERENCES

(1) Newman, S. Note on colloidal dispersions from block copolymers. *J. Appl. Polym. Sci.* **1962**, *6*, S15−S16.
(2) Krause, S. Dilute solution properties of a styrene - methyl methacrylate block copolymer. *J. Phys. Chem.* **1964**, *68*, 1948−1955.
(3) Tuzar, Z.; Kratochvíl, P. Block and graft copolymer micelles in solution. *Adv. Colloid Interface Sci.* **1976**, *6*, 201−232.
(4) Gao, Z.; Eisenberg, A. A model of micellization for block copolymers in solutions. *Macromolecules* **1993**, *26*, 7353−7360.
(5) Noolandi, J.; Hong, K. M. Theory of block copolymer micelles in solution. *Macromolecules* **1983**, *16*, 1443−1448.
(6) Förster, S.; Antonietti, M. Amphiphilic block copolymers in structure-controlled nanomaterial hybrids. *Adv. Mater.* **1998**, *10*, 195−217.

DOI: 10.1021/acs.langmuir.5b01651
Langmuir 2015, 31, 8764−8773

(7) Zhang, L.; Eisenberg, A. Multiple Morphologies of ″Crew-Cut″ Aggregates of Polystyrene-b-poly(acrylic acid) Block Copolymers. *Science* **1995**, *268*, 1728−1731.
(8) Zhang, L.; Eisenberg, A. Multiple Morphologies and Characteristics of "Crew-Cut" Micelle-like Aggregates of Polystyrene-b-poly(acrylic acid) Diblock Copolymers in Aqueous Solutions. *J. Am. Chem. Soc.* **1996**, *118*, 3168−3181.
(9) Gao, Z.; Varshney, S. K.; Wong, S.; Eisenberg, A. Block Copolymer ″Crew-Cut″ Micelles in Water. *Macromolecules* **1994**, *27*, 7923−7927.
(10) Yu, K.; Eisenberg, A. Bilayer Morphologies of Self-Assembled Crew-Cut Aggregates of Amphiphilic PS-b-PEO Diblock Copolymers in Solution. *Macromolecules* **1998**, *31*, 3509−3518.
(11) Burnett, G.; Meares, P.; Paton, C. Styrene+ methyl methacrylate block copolymers. Part 2.—Behaviour in dilute solutions. *Trans. Faraday Soc.* **1962**, *58*, 737−746.
(12) Fielding, L. A.; Lane, J. A.; Derry, M. J.; Mykhaylyk, O. O.; Armes, S. P. Thermo-responsive diblock copolymer worm gels in non-polar solvents. *J. Am. Chem. Soc.* **2014**, *136*, 5790−5798.
(13) Fielding, L. A.; Derry, M. J.; Ladmiral, V.; Rosselgong, J.; Rodrigues, A. M.; Ratcliffe, L. P.; Sugihara, S.; Armes, S. P. RAFT dispersion polymerization in non-polar solvents: facile production of block copolymer spheres, worms and vesicles in n-alkanes. *Chemical Science* **2013**, *4*, 2081−2087.
(14) Dan, M.; Huo, F.; Zhang, X.; Wang, X.; Zhang, W. Dispersion RAFT polymerization of 4-vinylpyridine in toluene mediated with the macro-RAFT agent of polystyrene dithiobenzoate: Effect of the macro-RAFT agent chain length and growth of the block copolymer nano-objects. *J. Polym. Sci., Part A: Polym. Chem.* **2013**, *51*, 1573−1584.
(15) Houillot, L.; Bui, C.; Save, M.; Charleux, B.; Farcet, C.; Moire, C.; Raust, J.-A.; Rodriguez, I. Synthesis of Well-Defined Polyacrylate Particle Dispersions in Organic Medium Using Simultaneous RAFT Polymerization and Self-Assembly of Block Copolymers. A Strong Influence of the Selected Thiocarbonylthio Chain Transfer Agent. *Macromolecules* **2007**, *40*, 6500−6509.
(16) Higgins, J. S.; Dawkins, J. V.; Maghami, G. G.; Shakir, S. A. Study of micelle formation by the diblock copolymer polystyrene—b-(ethylene-co-propylene) in dodecane by small-angle neutron scattering. *Polymer* **1986**, *27*, 931−936.
(17) Stejskal, J.; Hlavatá, D.; Sikora, A.; Konňák, Č.; Pleštil, J.; Kratochvíl, P. Equilibrium and non-equilibrium copolymer micelles: polystyrene-block-poly (ethylene-co-propylene) in decane and in diisopropylether. *Polymer* **1992**, *33*, 3675−3685.
(18) Hlavatá, D.; Stejskal, J.; Pleštil, J.; Koňák, Č.; Kratochvíl, P.; Helmstedt, M.; Mio, H.; Laggner, P. Heat-induced transition of polystyrene- block-poly(ethylene-co-propylene) micelles in decane and in dioxane. *Polymer* **1996**, *37*, 799−805.
(19) Bahadur, P.; Sastry, N. V.; Marti, S.; Riess, G. Micellar behaviour of styrene—isoprene block copolymers in selective solvents. *Colloids Surf.* **1985**, *16*, 337−346.
(20) Bang, J.; Viswanathan, K.; Lodge, T. P.; Park, M. J.; Char, K. Temperature-dependent micellar structures in poly(styrene-b-isoprene) diblock copolymer solutions near the critical micelle temperature. *J. Chem. Phys.* **2004**, *121*, 11489−11500.
(21) McConnell, G. A.; Gast, A. P. Melting of ordered arrays and shape transitions in highly concentrated diblock copolymer solutions. *Macromolecules* **1997**, *30*, 435−444.
(22) Choi, S.-H.; Bates, F. S.; Lodge, T. P. Structure of Poly(styrene-b-ethylene-alt-propylene) Diblock Copolymer Micelles in Squalane. *J. Phys. Chem. B* **2009**, *113*, 13840−13848.
(23) Hillmyer, M. A.; Lodge, T. P. Synthesis and self-assembly of fluorinated block copolymers. *J. Polym. Sci., Part A: Polym. Chem.* **2002**, *40*, 1−8.
(24) Szwarc, M.; Levy, M.; Milkovich, R. Polymerization initiated by electron transfer to monomer-a new method of formation of block polymers. *J. Am. Chem. Soc.* **1956**, *78*, 2656−2657.
(25) Szwarc, M. Living Polymers. *Nature* **1956**, *178*, 1168−1169.
(26) Mountrichas, G.; Mpiri, M.; Pispas, S. Micelles of star block (PSPI)8 and PSPI diblock copolymers (PS = polystyrene, PI = polyisoprene): structure and kinetics of micellization. *Macromolecules* **2005**, *38*, 940−947.
(27) Mandema, W.; Zeldenrust, H.; Emeis, C. A. Association of block copolymers in selective solvents, 1. Measurements on hydrogenated poly(styrene-isoprene) in decane and in trans-decalin. *Makromol. Chem.* **1979**, *180*, 1521−1538.
(28) Schouten, M.; Dorrepaal, J.; Stassen, W. J. M.; Vlak, W. A. H. M.; Mortensen, K. Thermal stability of polystyrene-b-poly(ethylene/propylene) diblock copolymer micelles in paraffinic solvents. *Polymer* **1989**, *30*, 2038−2046.
(29) Stacy, C. J.; Kraus, G. Micelle formation by butadiene-styrene block polymers in n-alkanes. *Polym. Eng. Sci.* **1977**, *17*, 627−633.
(30) Bang, J.; Jain, S.; Li, Z.; Lodge, T. P.; Pedersen, J. S.; Kesselman, E.; Talmon, Y. Sphere, cylinder, and vesicle nanoaggregates in poly(styrene-b-isoprene) diblock copolymer solutions. *Macromolecules* **2006**, *39*, 1199−1208.
(31) D'Oliveira, J. M. R.; Xu, R.; Jensma, T.; Winnik, M. A.; Hruska, Z.; Hurtrez, G.; Riess, G.; Martinho, J. M. G.; Croucher, M. D. Direct adsorption of polystyrene-poly(ethylene oxide) micelles in water onto polystyrene latex particles. *Langmuir* **1993**, *9*, 1092−1097.
(32) Kayes, J. B.; Rawlins, D. A. Adsorption characteristics of certain polyoxyethylene-polyoxypropylene block co-polymers on polystyrene latex. *Colloid Polym. Sci.* **1979**, *257*, 622−629.
(33) Evers, O. A.; Scheutjens, J. M. H. M.; Fleer, G. J. Statistical thermodynamics of block copolymer adsorption. Part 2. Effect of chain composition on the adsorbed amount and layer thickness. *J. Chem. Soc., Faraday Trans.* **1990**, *86*, 1333−1340.
(34) Awan, M. A.; Dimonie, V. L.; Filippov, L. K.; El-Aasser, M. S. Adsorption kinetics of amphipathic polystyrene-block-polybutadiene onto silicon wafer and polystyrene planar surfaces. *Langmuir* **1997**, *13*, 130−139.
(35) Marques, C.; Joanny, J. F.; Leibler, L. Adsorption of block copolymers in selective solvents. *Macromolecules* **1988**, *21*, 1051−1059.
(36) Shar, J. A.; Cosgrove, T.; Obey, T. M.; Warne, M. R.; Wedlock, D. J. Adsorption studies of diblock copolymers at the cyclohexane/carbon black interface. *Langmuir* **1999**, *15*, 7688−7694.
(37) Growney, D. J.; Mykhaylyk, O. O.; Armes, S. P. Micellization and adsorption behavior of a near-monodisperse polystyrene-based diblock copolymer in nonpolar media. *Langmuir* **2014**, *30*, 6047−6056.
(38) Growney, D. J.; Mykhaylyk, O. O.; Derouineau, T.; Fielding, L. A.; Smith, A. J.; Aragrag, N.; Lamb, G. D.; Armes, S. P. Star diblock copolymer concentration dictates the degree of dispersion of carbon black particles in non-polar media: bridging flocculation versus steric stabilization. *Macromolecules* **2015**, *48*, 3691−3704.
(39) Clague, A. D. H.; Donnet, J. B.; Wang, T. K.; Peng, J. C. M. A comparison of diesel engine soot with carbon black. *Carbon* **1999**, *37*, 1553−1565.
(40) Diatto, P.; Anzani, M.; Tinucci, L.; Tripaldi, G.; Vettor, A. Investigation on soot dispersant properties and wear effects in the boundary lubrication regime. *Tribology Series* **1999**, *36*, 809−819.
(41) Gautam, M.; Chitoor, K.; Durbha, M.; Summers, J. C. Effect of diesel soot contaminated oil on engine wear — investigation of novel oil formulations. *Tribol. Int.* **1999**, *32*, 687−699.
(42) Green, D. A.; Lewis, R. The effects of soot-contaminated engine oil on wear and friction: A review. *Proc. Inst. Mech. Eng., Part D* **2008**, *222*, 1669−1689.
(43) Adams, C. E.; Belmont, J. A.; Johnson, J. E. Ink jet ink formulations containing carbon black products. U.S. Patent 5,571,311, 1996.
(44) Ma, S.-H.; Matrick, H.; Shor, A. C.; Spinelli, H. J. Aqueous pigmented inks for ink jet printers. U.S. Patent 5,085,698, 1992.
(45) Carmine, J.; Ryntz, R. The Use of Naphthenic Acid Ester As a Dispersing Agent in Aqueous Conductive Primers. *J. Coat. Technol.* **1994**, *66*, 93−98.
(46) Mächtle, W. Characterization of dispersions using combined H_2O/D_2O ultracentrifuge measurements. *Makromol. Chem.* **1984**, *185*, 1025−1039.

DOI: 10.1021/acs.langmuir.5b01651
Langmuir 2015, 31, 8764−8773

(47) Lechner, M. D.; Mächtle, W. Determination of the Particle Size Distribution of 5−100-nm Nanoparticles with the Analytical Ultracentrifuge: Consideration and Correction of Diffusion Effects. In *Analytical Ultracentrifugation V*, Cölfen, H., Ed.; Springer: Berlin, 1999; Vol. *113*, pp 37−43.
(48) Planken, K. L.; Cölfen, H. Analytical ultracentrifugation of colloids. *Nanoscale* **2010**, *2*, 1849−1869.
(49) Cölfen, H.; Pauck, T. Determination of particle size distributions with angström resolution. *Colloid Polym. Sci.* **1997**, *275*, 175−180.
(50) Mächtle, W. High-Resolution, Submicron Particle Size Distribution Analysis Using Gravitational-Sweep Sedimentation. *Biophys. J.* **1999**, *76*, 1080−1091.
(51) Detloff, T.; Sobisch, T.; Lerche, D. Particle Size Distribution by Space or Time Dependent Extinction Profiles obtained by Analytical Centrifugation. *Particle & Particle Systems Characterization* **2006**, *23*, 184−187.
(52) Sobisch, T.; Lerche, D. Thickener performance traced by multisample analytical centrifugation. *Colloids Surf., A* **2008**, *331*, 114−118.
(53) Demeler, B.; Nguyen, T.-L.; Gorbet, G. E.; Schirf, V.; Brookes, E. H.; Mulvaney, P.; El-Ballouli, A. a. O.; Pan, J.; Bakr, O. M.; Demeler, A. K.; Hernandez Uribe, B. I.; Bhattarai, N.; Whetten, R. L. Characterization of Size, Anisotropy, and Density Heterogeneity of Nanoparticles by Sedimentation Velocity. *Anal. Chem.* **2014**, *86*, 7688−7695.
(54) Carney, R. P.; Kim, J. Y.; Qian, H.; Jin, R.; Mehenni, H.; Stellacci, F.; Bakr, O. M. Determination of nanoparticle size distribution together with density or molecular weight by 2D analytical ultracentrifugation. *Nat. Commun.* **2011**, *2*, 335.
(55) Lerche, D.; Sobisch, T. Consolidation of concentrated dispersions of nano- and microparticles determined by analytical centrifugation. *Powder Technol.* **2007**, *174*, 46−49.
(56) Krpetić, Ž.; Davidson, A. M.; Volk, M.; Lévy, R.; Brust, M.; Cooper, D. L. High-Resolution Sizing of Monolayer-Protected Gold Clusters by Differential Centrifugal Sedimentation. *ACS Nano* **2013**, *7*, 8881−8890.
(57) Balmer, J. A.; Le Cunff, E. C.; Armes, S. P.; Murray, M. W.; Murray, K. A.; Williams, N. S. J. When Does Silica Exchange Occur between Vinyl Polymer−Silica Nanocomposite Particles and Sterically Stabilized Latexes? *Langmuir* **2010**, *26*, 13662−13671.
(58) Fielding, L. A.; Mykhaylyk, O. O.; Armes, S. P.; Fowler, P. W.; Mittal, V.; Fitzpatrick, S. Correcting for a Density Distribution: Particle Size Analysis of Core−Shell Nanocomposite Particles Using Disk Centrifuge Photosedimentometry. *Langmuir* **2012**, *28*, 2536−2544.
(59) Colard, C. A. L.; Teixeira, R. F. A.; Bon, S. A. F. Unraveling Mechanistic Events in Solids-Stabilized Emulsion Polymerization by Monitoring the Concentration of Nanoparticles in the Water Phase. *Langmuir* **2010**, *26*, 7915−7921.
(60) Yow, H. N.; Biggs, S. Probing the stability of sterically stabilized polystyrene particles by centrifugal sedimentation. *Soft Matter* **2013**, *9*, 10031−10041.
(61) Monopoli, M. P.; Walczyk, D.; Campbell, A.; Elia, G.; Lynch, I.; Baldelli Bombelli, F.; Dawson, K. A. Physical−Chemical Aspects of Protein Corona: Relevance to in Vitro and in Vivo Biological Impacts of Nanoparticles. *J. Am. Chem. Soc.* **2011**, *133*, 2525−2534.
(62) Au, K. M.; Armes, S. P. Heterocoagulation as a Facile Route To Prepare Stable Serum Albumin-Nanoparticle Conjugates for Biomedical Applications: Synthetic Protocols and Mechanistic Insights. *ACS Nano* **2012**, *6*, 8261−8279.
(63) Detloff, T.; Sobisch, T.; Lerche, D. Particle size distribution by space or time dependent extinction profiles obtained by analytical centrifugation (concentrated systems). *Powder Technol.* **2007**, *174*, 50−55.
(64) Lascelles, S. F.; Armes, S. P. Synthesis and characterization of micrometre-sized, polypyrrole-coated polystyrene latexes. *J. Mater. Chem.* **1997**, *7*, 1339−1347.
(65) Stejskal, J.; Kratochvíl, P.; Armes, S. P.; Lascelles, S. F.; Riede, A.; Helmstedt, M.; Prokeš, J.; Křivka, I. Polyaniline Dispersions. 6. Stabilization by Colloidal Silica Particles. *Macromolecules* **1996**, *29*, 6814−6819.
(66) Lovett, J. R.; Fielding, L. A.; Armes, S. P.; Buxton, R. One-Pot Preparation of Conducting Polymer-Coated Silica Particles: Model Highly Absorbing Aerosols. *Adv. Funct. Mater.* **2014**, *24*, 1290−1299.
(67) Chiu, H.-T.; Chang, C.-Y.; Chiang, T.-Y.; Kuo, M.-T.; Wang, Y.-H. Using analytical centrifugation to characterize the dispersibility and particle size distributions of organic/inorganic composite coatings. *J. Polym. Res.* **2011**, *18*, 1587−1596.
(68) Chiu, H.-T.; Chiang, T.-Y.; Huang, Y.-C.; Chang, C.-Y.; Kuo, M.-T. Preparation, Particle Characterizations and Application of Nano-Pigment Suspension. *Polym.-Plast. Technol. Eng.* **2010**, *49*, 1552−1562.
(69) Petzold, G.; Goltzsche, C.; Mende, M.; Schwarz, S.; Jaeger, W. Monitoring the stability of nanosized silica dispersions in presence of polycations by a novel centrifugal sedimentation method. *J. Appl. Polym. Sci.* **2009**, *114*, 696−704.
(70) Scares, B. G.; de Souza Gomes, A. Spectrophotometric determination of the styrene content of alpha-methylstyrene—styrene copolymers. *Polym. Bull.* **1988**, *20*, 543−548.
(71) Godward, J.; Heatley, F.; Price, C. 1 H Nuclear magnetic relaxation study of the phase structure of polystyrene-block-poly (ethylene/propylene) copolymer micelles. *J. Chem. Soc., Faraday Trans.* **1993**, *89*, 3471−3475.
(72) Pedersen, J. S.; Svaneborg, C.; Almdal, K.; Hamley, I. W.; Young, R. N. A small-angle neutron and X-ray contrast variation scattering study of the structure of block copolymer micelles: Corona shape and excluded volume interactions. *Macromolecules* **2003**, *36*, 416−433.
(73) Rieker, T. P.; Misono, S.; Ehrburger-Dolle, F. Small-angle X-ray scattering from carbon blacks: crossover between the fractal and porod regimes. *Langmuir* **1999**, *15*, 914−917.
(74) Sahouli, B.; Blacher, S.; Brouers, F.; Darmstadt, H.; Roy, C.; Kaliaguine, S. Surface morphology and chemistry of commercial carbon black and carbon black from vacuum pyrolysis of used tyres. *Fuel* **1996**, *75*, 1244−1250.
(75) Pedersen, J. S.; Svaneborg, C.; Almdal, K.; Hamley, I. W.; Young, R. N. A small-angle neutron and X-ray contrast variation scattering study of the structure of block copolymer micelles: corona shape and excluded volume interactions. *Macromolecules* **2003**, *36*, 416−433.

DOI: 10.1021/acs.langmuir.5b01651
Langmuir 2015, 31, 8764−8773